Dependence of Skin Permeability on Contact Area

Pankaj Karande[1] and Samir Mitragotri[1,2]

Received September 23, 2002; accepted October 8, 2002

Purpose. We report that experimentally measured skin permeability to hydrophilic solutes increases with decreasing contact area between the formulation and the skin. Our results suggest that an array of smaller reservoirs should thus be more effective in increasing transdermal drug delivery compared to a large single reservoir of the same total area.

Methods. Experimental assessment of the dependence of skin permeability on reservoir size was performed using two model systems, an array of liquid reservoirs with diameters in the range of 2 mm to 6 mm and an array of gel disk reservoirs with diameters in the range of 3 mm to 16 mm. Full thickness pig skin was used as an experimental model. Two molecules, sodium lauryl sulfate (SLS) and oleic acid, were used as model penetration enhancers.

Results. Mannitol transport per unit area into and across the skin increased with a decrease in the contact area between the skin and the formulation. Mannitol permeability increased approximately 6-fold with a decrease in the reservoir size from 16 mm to 3 mm in presence of 0.5% SLS in PBS (phosphate buffered saline) as a permeability enhancer. Similar results were obtained when oleic acid was used as an enhancer.

Conclusions. To explain the observed dependence of transdermal transport on contact area a simple mathematical model based on skin geometry in the reservoir was developed. The model predicts a lateral strain in the skin due to preferential swelling of skin upon penetration of water. We propose that this lateral strain is responsible for the increased skin permeability at lower reservoir sizes.

KEY WORDS: transdermal; array; hydration; gradient; stress; strain.

INTRODUCTION

Transdermal Drug Delivery (TDD) offers an advantageous mode of drug administration in that it eliminates first pass metabolism and provides for a sustained release of drugs for a prolonged period of time. However, low skin permeability still poses severe limitations in utilizing TDD. Designed to impede the influx of toxic substances into the body, skin offers a very low permeability to the movement of foreign molecules across it. Only a handful of molecules are being delivered using the transdermal route. Low skin permeability originates from a unique hierarchical structure where strata of differing transport barriers are stacked together. The superficial layer of skin (15 μm thick) stratum corneum (SC) forms the primary barrier with a high transport resistance. SC consists of several layers of keratinocytes within which lipid bilayers are stacked (1). Overcoming this barrier safely and reversibly is a fundamental problem that persists today in the field of transdermal delivery.

Several technologic advances have been made in the past couple of decades to overcome this barrier. Iontophoresis, sonophoresis, and use of chemical enhancers are a few to name (2–5). We report a novel finding in this study that may be used to increase the flux of molecules across the skin by modifying reservoir geometry rather than formulation chemistry. Specifically, we report that transdermal transport of hydrophilic solutes can be enhanced by using an array of donor reservoirs rather than a single large reservoir. Fundamentally, this enhancement originates from our finding that skin permeability exhibits an inverse dependence on skin area in contact with the formulation. In this article, we first provide the experimental data on the effect of formulation reservoir size on skin permeability and then discuss our hypothesis of the underlying mechanisms using a simple mathematical treatment based on the geometry of the skin in the reservoir.

MATERIALS AND METHODS

Transport Measurements Using a Liquid Reservoir Array

Transdermal transport experiments were performed using porcine skin. Skin was harvested from pigs and was stored at –70°C until the time of experiments. Skin was thawed at room temperature and was placed in a PBS receiver fluid (10 ml) such that PBS contacted the skin on all sides and the bottom but not the top (Fig. 1A). To assess the effect of contact area on skin permeability, an array of liquid reservoirs was created. This array was created by punching holes in a square pattern in a polyurethane slab (thickness ~5 mm) such that the total skin area exposed to the formulation in the reservoirs was ~2 cm^2. These reservoirs were separated from each other by one diameter. Such arrays were made for different size reservoirs (diameters in the range of 2–6 mm, contact area per reservoir in the range 0.03–0.3 cm^2). The top surface of the skin was dried of any surface moisture. The array was then mounted on the skin using an adhesive. Note that no clamping was required to attach the reservoirs to the skin. Lateral diffusion of formulation in the polyurethane slab was restricted by coating inner walls of the reservoirs with silicone for 24 h.

Transdermal transport experiments were performed using mannitol (American Radiolabeled Chemicals, St. Louis, MO) as a model solute and sodium lauryl sulfate (SLS) (Fisher Scientific, Fairlawn, NJ) as a model enhancer. Added as a tracer to the formulation (0.5% SLS in PBS) was 10 μCi/ml of ^3H labeled mannitol. The formulation was then added to the different reservoirs. Excellent sealing was obtained between the polyurethane array and the skin and no leakage of formulations was observed. The reservoir array was placed on the skin for 24 h. The receiver compartment was sampled at the end of 24 h to calculate the amount of mannitol delivered across the skin into the PBS. Permeability of skin exposed to formulations in different reservoirs was calculated for each reservoir size by dividing the total amount delivered by the number of reservoirs, area of each reservoir, contact time, and mannitol concentration in each reservoir. Amount of mannitol delivered into the skin was also measured by dissolving the skin using a tissue and gel solubilizer (0.5 M Solvable, Packard Bioscience, TH, Groningen).

[1] Department of Chemical Engineering University of California, Santa Barbara, California 93106.

[2] To whom correspondence should be addressed. (e-mail: samir@engineering.ucsb.edu)

0724-8741/03/0200-0257/0

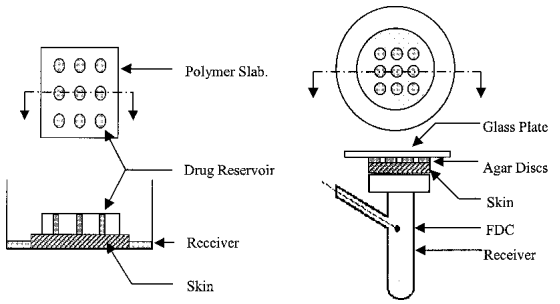

Fig. 1. A) Schematic of the drug reservoir arrangement in a polyurethane slab. The formulation is filled in the holes punched in the slab. The polymer slab is placed on the skin, which is held in a known volume of PBS. The mannitol permeating through the skin is sampled from the PBS in the receiver. **B)** Schematic of the agar gel disk assembly on the skin in a Franz diffusion cell (FDC). The skin is held on top of the receiver compartment of the FDC supported on a mesh. The drug disks are placed on top of the skin. A glass plate is placed on top of the disks to achieve good contact between the skin and disks. The mannitol permeating through the skin is sampled from the PBS in the receiver.

Transport Measurements Using Agar Disk Arrays

A second experimental system was used to assess the dependence of permeability on contact area. In this system, permeation of mannitol from gel disks was studied. For this purpose, agar gel disks were prepared by dissolving 0.5 gm agar (Becton Dickinson Microbiology Systems, Sparks, MD) in 20 ml of 0.5% (w/v) SLS in PBS. Added to the mixture was 10 μCi/ml ^{3}H radiolabeled mannitol. The mixture was heated until agar formed a viscous solution. The viscous mixture was allowed to settle into a gel by pouring it into a petri dish to form a circular disk of 3.5 mm thickness. Disks of various diameters (16, 9, 5, and 3 mm) were cut using a leather punch. These disks were then placed in a square array pattern on the skin, similar to the liquid reservoirs, atop Franz Diffusion Cells (PermeGear Inc., Bethlehem, PA). A steel mesh was placed underneath the skin for support. A glass cover slide was placed above the disks to ensure good contact of skin with the disks. A schematic of this assembly is depicted in Fig. 1B. Receiver compartments of the FDC were sampled at the end of 24 h and concentration of radiolabeled mannitol in these samples was measured using a scintillation counter (Packard Tri-Carb 2100TR, Packard Instrument Company, Meriden, CT). Permeability of skin in each reservoir was calculated by dividing the total flux obtained by the number of reservoirs at that particular size, the single reservoir area and concentration of the formulation in the agar disks. Amount of mannitol delivered into the skin was also measured by dissolving the skin using a tissue and gel solubilizer (0.5 M Solvable, Packard Bioscience, TH, Groningen).

RESULTS

Skin permeability to mannitol increased with decreasing contact area in both types of test geometries (that is, liquid reservoirs and agar gels). Figure 2 shows the dependence of skin mannitol permeability measured using liquid reservoirs (relative to that from the largest reservoir [6 mm], where the permeability was 1.4×10^{-4} cm/hr) as a function of the reciprocal reservoir radius, $1/r$, for seven different reservoir sizes (6 mm, 5 mm, 4 mm, 3.5 mm, 3 mm, 2.5 mm and 2 mm, all numbers are diameters). Figure 3A shows a similar dependence of mannitol permeability measured using gel disks (relative to that from the largest disk [16 mm], where the permeability was 1.2×10^{-4} m/hr) for varying reservoir diameters (16 mm, 9 mm, 5 mm and 3 mm). In both cases (Figs. 2 and 3A), a significant increase in permeability is observed with a decrease in contact area. The overall increase in permeability with reservoir size is comparable in both systems, thus confirming that the dependence of permeability on contact area is not an artifact of any particular experimental system.

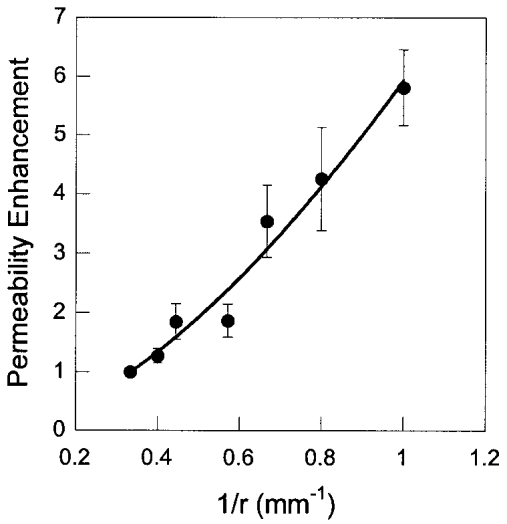

Fig. 2. The dependence of skin permeability (relative to that from a 6 mm reservoir) in a liquid reservoir polyurethane array of reservoir diameters 2, 2.5, 3, 3.5, 4, 5, and 6 mm in presence of 0.5% SLS in PBS (r = radius in mm). Skin permeability increases with decreasing reservoir size to up to 6 fold in a 2 mm reservoir as compared to a 6 mm reservoir. The solid line is used to visually capture the trend and has not been fitted to the data. Error bars correspond to SD (n = 3). Actual permeability values corresponding to the different reservoir diameters are: 6 mm ($1.4 \pm 0.08 \times 10^{-4}$ cm/hr), 5 mm ($1.8 \pm 0.18 \times 10^{-4}$ cm/hr), 4 mm ($2.6 \pm 0.42 \times 10^{-4}$ cm/hr), 3.5 mm ($2.7 \pm 0.4 \times 10^{-4}$ cm/hr), 3 mm ($5.1 \pm 0.88 \times 10^{-4}$ cm/hr), 2.5 mm ($6.2 \pm 1.3 \times 10^{-4}$ cm/hr) and 2 mm ($8.4 \pm 0.93 \times 10^{-4}$ cm/hr).

To confirm that the dependence of skin permeability on reservoir diameter is not specific to SLS, experiments were performed using gel disks where SLS was replaced by 1.0% oleic acid in a 1:1 PBS: Ethanol solution. Figure 3B shows the results of these experiments, where skin permeability to mannitol (relative to that from a 16 mm disk, where the permeability was 3.6×10^{-5} cm/hr) is plotted at varying reservoir sizes. The data obtained for oleic acid show the same trend as that observed with SLS. The magnitudes of enhancement are different for the two systems (SLS and oleic acid) and are determined by their individual dynamics in skin. However Fig. 3B reinforces the generality of the observations reported in Figs. 2 and 3A. To verify that the observed effect is not specific to mannitol we repeated these experiments with inulin as a model solute (Data shown in Table IA). Furthermore, experiments were performed in the absence of enhancers (that is, in the presence of PBS alone) and mannitol as a model solute (Data shown in Table IB). The dependence of permeability on reservoir size in both cases was comparable to that shown in Figs. 2 and 3.

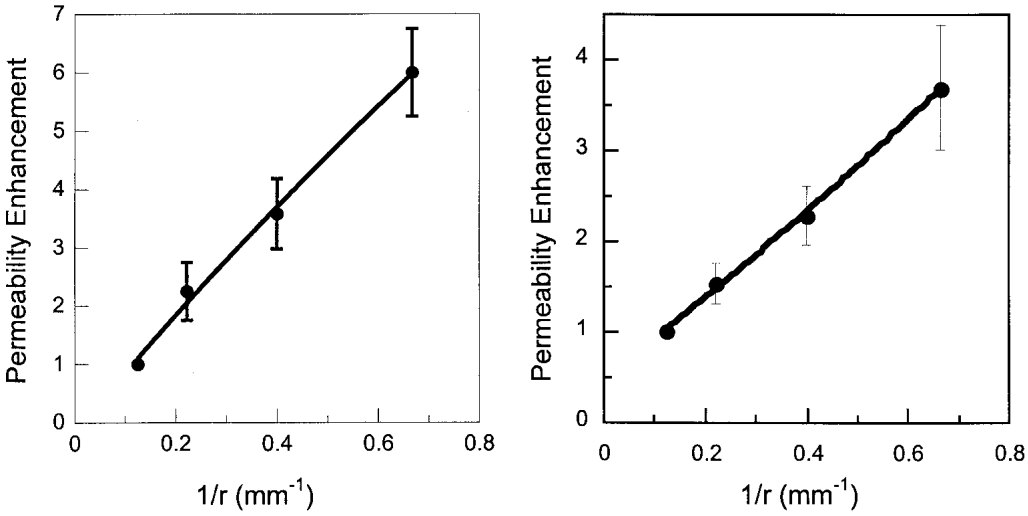

Fig. 3. A: The dependence of skin permeability (relative to that from a 16 mm disk) on reciprocal of reservoir radius in the agar gel disk assembly for 0.5% SLS. The permeability increases with a decrease in the reservoir size. All enhancement factors have been normalized to the enhancement obtained at the largest reservoir size in the setup (16 mm). The solid line is used to visually capture the trend. Error bars correspond to one standard deviation (n = 5). Actual permeability values corresponding to the different reservoir sizes are: 16 mm (1.2 ± 0.01 × 10^{-4} cm/hr), 9 mm (2.7 ± 0.60 × 10^{-4} cm/hr), 5 mm (4.3 ± 0.72 × 10^{-4} cm/hr), 3 mm (7.2 ± 0.90 × 10^{-4} cm/hr). B: The dependence of skin permeability (relative to that from a 16 mm disk) on reciprocal of reservoir size in the agar gel disk assembly for 1% Oleic acid. The enhancement factors increase with a decrease in the reservoir size. All enhancement factors have been normalized to the enhancement obtained at the largest reservoir size in the setup (16 mm). The solid line is used to visually capture the trend. Error bars correspond to one standard deviation (n = 3). Actual permeability values corresponding to the different reservoir sizes are: 16 mm (0.36 ± 0.00 × 10^{-4} cm/hr), 9 mm (0.56 ± 0.08 × 10^{-4} cm/hr), 5 mm (0.83 ± 0.12 × 10^{-4} cm/hr), 3 mm (1.4 ± 0.26 × 10^{-4} cm/hr).

DISCUSSION

According to Fick's law, skin permeability is independent of the contact area between the skin and the formulation. However, we hypothesize that this assumption, though valid for large skin areas (>1 cm^2) needs careful consideration when the contact area between skin and formulation is small. Specifically, we propose that for small contact areas, selective swelling of the skin due to penetration of solvent induces strains in the stratum corneum, thereby increasing the permeability of the skin. Since water is the primary constituent of the formulations discussed in this study, swelling induced by water penetration or hydration is of primary concern in this study. Swelling of skin exposed to aqueous formulations in the reservoir arrays can be seen in Fig. 4A which shows a cross section of porcine skin exposed to PBS in a 3 mm reservoir array for 24 h. Analysis of the strain induced by selective swelling of the skin is presented in the following section.

Table I. A) Permeability Values for Inulin from 0.5% SLS in Gel Disk Arrays. Each Number is an Average of Three Experiments. B) Summary of Permeability Values in Liquid Reservoir Arrays Containing PBS alone in the Absence of Any Enhancer. Each Number Is an Average of Three Experiments

Reservoir diameter (mm)	Inulin permeability from 0.5% SLS (× 10^4 cm/h)
16	0.065 ± 0.00
9	0.12 ± 0.012
5	0.27 ± 0.042
3	0.34 ± 0.033

Table IA

Reservoir diameter (mm)	Mannitol permeability from PBS (× 10^4 cm/h)
6	0.76 ± 0.27
5	0.84 ± 0.01
4	0.72 ± 0.03
3.5	0.64 ± 0.11
3	1.22 ± 0.40
2.5	0.84 ± 0.01
2	1.67 ± 0.30

Table IB

Effects of hydration on skin permeability have been extensively studied (6–12). Skin mechanical properties (elasticity and plasticity) as well as permeability are known to be dependent on the relative water content or hydration state of the SC (6), (8–10), (12–13). Although mechanisms of hydration-mediated permeability are not fully clear, swelling of stratum corneum and fluidization of lipid bilayers are believed to be responsible for this phenomenon (10–11), (14–16). Increase in the stratum corneum thickness by as much as 26% due to water absorption has been reported (7). Increase in skin volume should induce internal stresses, especially in keratin fibers, which need to enlarge to accommodate absorbed water. For large skin areas (>1cm^2), swelling is unlikely to induce significant strains, however, the following analysis will show that selective swelling of a small section of skin may induce significant strains.

Consider a flat, circular piece of skin of full thickness h, placed in a diffusion cell of radius r, as shown in Fig. 4B. Upon fully hydrating, the skin swells with an increase in its thickness by Δh. The skin, which was flat prior to hydration, now assumes the shape of an oblate spheroidal cap, defined by major axis r and minor axis Δh. The surface area of the hydrated skin is given by the following equation.

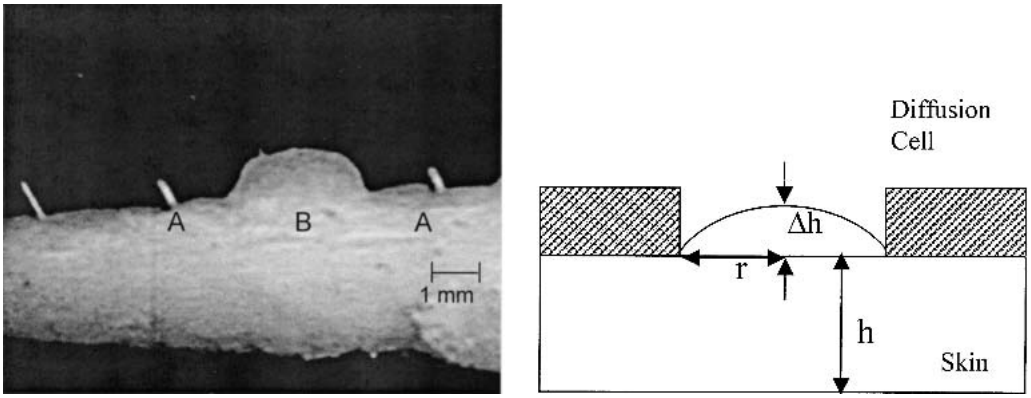

Fig. 4. A: An image showing a skin piece held in a polyurethane array for 24 h mounted in the diffusion cell. The skin exposed to PBS is swollen due to hydration (B). The array was mounted in the diffusion cell to clearly bring out the swelling of the skin due to hydration. Swelling in the set-up shown in Fig. 1A is qualitatively similar but quantitatively smaller. B: A schematic representation of skin swollen due to hydration as shown in Fig. 4A. The skin swells due to hydration from an original thickness of h to $h+\Delta h$. The base radius stays constant at r. The swollen part of the skin can be treated as an oblate spheroid of major axis r and minor axis Δh.

$$A_{hydrated} = \pi\left(r^2 + \frac{\Delta h^2}{2e}\ln\left(\frac{1+e}{1-e}\right)\right) \quad [1]$$

where, e, is the eccentricity of the spheroid and is given by the following equation.

$$e^2 = 1 - \frac{\Delta h^2}{r^2} \quad (2)$$

Noting that the skin area prior to hydration was πr^2, the change in SC area after hydration, ΔA, is given by the following equation.

$$\Delta A = A_{hydrated} - A_{unhydrated} = \pi\frac{\Delta h^2}{2e}\ln\left(\frac{1+e}{1-e}\right) \quad (3)$$

The strain (fractional increase in area) induced in the SC due to hydration, ε, is then given by the following equation.

$$\varepsilon = \frac{\Delta A}{A_{unhydrated}} = \frac{1}{2e}\left(\frac{\Delta h}{r}\right)^2\ln\left(\frac{1+e}{1-e}\right) \quad (4)$$

Since the strain, ε, corresponds to the change in surface area of the skin, it essentially indicates the elongation experienced by the stratum corneum. Note that Δh is the change in skin thickness due to hydration and is an intrinsic characteristic of the skin. That is, Δh does not depend on skin area. This can be shown with the help of a simple mathematical treatment of the oblate spheroidal cap. Specifically, the volume of the swollen skin is given by the following equation.

$$V_{cap} = \frac{2}{3}\pi r^2\,\Delta h + \pi r^2 h \quad (5)$$

where, $\pi r^2 h$ is the volume of skin prior to hydration. The increase in skin volume due to hydration can be calculated as follows:

$$\Delta V = V_{hydrated} - V_{unhydrated} = \frac{2}{3}\pi r^2\,\Delta h \quad [6]$$

The change in skin volume per unit area, γ, is then given by the following equation.

$$\gamma = \left(\frac{\Delta V}{A}\right) = \left(\frac{\Delta V}{\pi r^2}\right) = \frac{2}{3}\Delta h \quad [7]$$

Thus Δh represents change in skin volume per unit area on hydration, which is an intrinsic characteristics of skin. It simply describes the capacity of skin to absorb water. Then, γ is just a physical constant that can be determined experimentally. For this purpose, we hydrated full thickness porcine skin possessing different areas in the range of 0.36 cm^2 to 20 cm^2 with PBS. Skin was typically 4 mm thick. The skin was thawed at room temperature in open air for 24 h and its mass, m_o, was measured. The skin was then hydrated in excess phosphate buffered saline (PBS) for 24 h and its mass, m_h, was measured again. The amount of water absorbed by the skin, Δm, was calculated ($\Delta m = m_h - m_o$). The change in skin volume per unit area, γ, was the calculated using the following equation, $\gamma = \Delta m/\rho A$, where ρ is the density of PBS (1 g/cm^3). Over the range of skin areas studied, γ was indeed found to be constant and was found to be 0.58 ± 0.1 mm (the uncertainty in the value of γ, 0.1 mm, is denoted as $\delta\gamma$). This value of γ was used to calculate Δh which was found to be 0.87 mm. Effectively, even though the skin exhibits the same change in thickness at different reservoir sizes, this increase occurs over considerably different skin areas at different reservoir sizes.

Given that Δh is a constant, Eq. (4) predicts that the strain induced by hydration varies inversely with the area of the skin. For large skin areas (r ~1 cm, that is $r >> \Delta h$), the hydration strain, ε, is relatively small and may be nonconsequential to transdermal drug transport. However, for smaller values of r, the strain induced by hydration can be significant and may affect transdermal drug transport. Increased strain is expected to increase skin permeability through structural alterations. Accordingly, skin permeability, P, is expected to increase with a decrease in the radius of its contact with the formulation, r, as:

$$P = F(\varepsilon) = G\left(\frac{\Delta h^2}{r^2}\right) \sim f\left(\frac{1}{r}\right) \quad [8]$$

where, f is a function whose exact dependence cannot be determined from the first principles at this point.

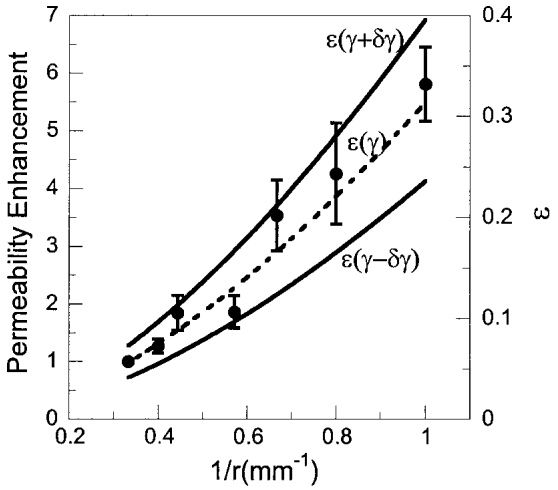

Fig. 5. The dependence of skin permeability enhancement on reciprocal of reservoir radius in the polyurethane slab reservoir assembly for 0.5% SLS and the theoretically calculated area strain, ε on reservoir radius r. Strain is non consequential to the transdermal delivery at large reservoir sizes (r > 10 mm). The strain can be as high as 80% at a reservoir radius of 0.5 mm. The dotted line represents the theoretically calculated area strain, ε, at the reservoir sizes used in the experiments. The solid lines ε ($\gamma + \delta\gamma$) and ε ($\gamma - \delta\gamma$) represent the area strains calculated based on the uncertainty in the experimental determination of γ ($\delta\gamma$). All enhancement factors have been normalized to the enhancement obtained at the largest reservoir size in the setup (6 mm).

Dependence of lateral strain, ε, on reservoir radius predicted by Eq. (4) is plotted in Fig. 5 (dotted line). Experimental data on permeability from various reservoir sizes (reproduced from Fig. 2) are also shown (closed circles). The overall dependence of enhancement on $1/r$ is comparable to that of ε. Note that a comparison of the dependence of enhancement on $1/r$ with that of ε on $1/r$ should be performed at a qualitative level since no quantitative relationship between enhancement and ε is proposed at this point. The uncertainty in calculating ε is based on $\delta\gamma$, the error in the change in skin volume per unit area due to hydration. Here, $|\delta\gamma|$ is 0.1 mm as discussed earlier. The solid lines in Fig. 5 represent ε plotted for ($\gamma + \delta\gamma$) and ($\gamma - \delta\gamma$). It is interesting to note that the uncertainty in the enhancement factors at each reservoir size (error bars on closed circles) scales as the uncertainty in calculating, theoretically, the strain in the skin based on experimentally determined γ.

Figure 5 shows that the predicted dependence of ε on $1/r$ is non-linear. In addition, the figure shows that for relatively large reservoir diameters, say 5–10 mm, the area strain in the skin is indeed small (less than 5%). However, as the reservoir size decreases below 5 mm, the strain increases rapidly and approaches a value of 82% as the reservoir diameter approaches 1 mm (For a reservoir with a diameter of 2 mm, the smallest reservoir diameter used in experiments, the strain is ~30%). A strain of ~80% is very high and may induce significant structural changes in the skin. Fundamentally, the strain arises from the fact that the skin thickness increases by Δh in the hydrated region. However, since the skin is essentially hinged at the periphery, the strain becomes particularly significant as Δh approaches r.

To further confirm that swelling of skin in the area exposed to formulations is indeed related to selective hydration in these regions, we measured the water content in the skin directly underneath the reservoir and that in the region surrounding the reservoir. Single reservoir templates were created at different reservoir diameters (5 mm, 4 mm, 3.5 mm, 3 mm, 2.5 mm, and 2 mm). Penetration of ^{3}H water from the

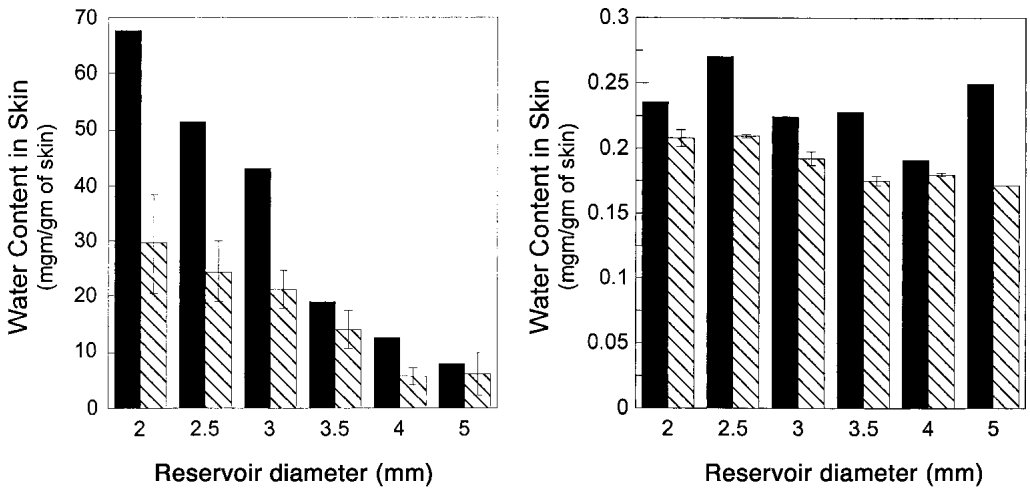

Fig. 6. A: Hydration gradient in skin pieces exposed to PBS in various reservoirs. Solid bars indicate the water content (measured using ^{3}H water) directly under the reservoir and the crossed bars indicate the water content in the surrounding skin. The difference in heights of the solid bar and the crossed bar at each reservoir size (hydration or strain gradient) increases with the decrease in the reservoir size. Error bars correspond to SD (n = 8–10). B: Hydration gradient in skin pieces at different reservoir sizes when exposed to propylene glycol. Solid bars indicate the water content (measured using ^{3}H water) directly under the reservoir and the crossed bars indicate the water content in the surrounding skin. There is no significant difference between the solid bar and the crossed bar at each reservoir size indicating that there is no strain gradient introduced by propanediol. Absence of a strain gradient results in a constant permeability over the entire range of reservoir sizes. Error bars correspond to n = 8–10.

reservoir into skin directly underneath the skin as well as that in the skin in the neighboring region was measured at the end of 24 h by taking punch biopsies in these regions and counting the amount of ^{3}H water in these samples. These data are shown in Fig. 6A. At each reservoir size (x axis) the solid bars represent water content per unit weight of skin (gm) directly underneath the reservoir. The hatched bars represent the same quantity calculated in the region of skin surrounding the reservoir. Two characteristic features of these data are clear from Fig. 6A. First, the hydration level of skin directly underneath the reservoir is significantly greater than that in the surrounding region. Second, the difference between the two bars grows with a decrease in the reservoir size. In other words, the difference in the hydration levels of skin directly underneath the formulation and the surrounding skin, grows with decreasing reservoir size. This result is in agreement with our hypothesis: water penetration swells the skin resulting in a strain across the SC that increases with decreasing reservoir size. A corollary to this hypothesis would be: a solvent, which does not swell the skin, does not exhibit increased permeability with reduction in reservoir size. Using exactly the same experimental assembly as discussed above we repeated experiments using propylene glycol. Propylene glycol was selected based on our preliminary observations that it does not swell the skin by penetration. These data, plotted in Fig. 6B, show no significant difference between the solid and hatched bars. Based on the numbers presented in Fig. 6A we also calculated the change in skin thickness due to the swelling. The change in the skin volume per unit area for the smallest reservoir (2 mm diameter) was found to be 0.2 mm, comparable to the value 0.58 mm as obtained in the skin hydration experiments discussed earlier. This reconfirms our belief that skin swelling is a function, only, of the hydration rate and not the total skin area exposed to the formulation.

The prediction that strain in the skin increases with a decrease in contact area is not necessarily restricted to swelling due to water. Any solvent, which can induce swelling of skin, can potentially exhibit a similar phenomenon. However, the magnitude of the strain will be different for each solvent. In addition any other mechanism that may create selective swelling of the skin, for e.g., application of vacuum (suction) to selective regions of skin may exhibit similar behavior (17). It is important to note that the strain induced in the skin depends on the absolute value of Δh and not the relative increase in thickness, that is, $\Delta h/h$. Since the value of Δh will vary for each experimental model system, for example, heat-stripped epidermis, dermatomed skin, or *in vivo* skin, the extent to which this effect is observed in other experimental systems needs to be determined.

The inverse dependence of permeability on reservoir size has been previously discussed in the context of edge damage. However, the mechanism discussed here is completely different from the classic "edge damage" hypothesis, which assumes that clamping of the skin in a diffusion cell damages the skin due to mechanical pressure (18–20). The length per unit area in these systems, damaged due to clamping, increases as the reservoir area decreases and hence skin permeability increases at a lowered area. Since mechanical edge damage is trivial in this study, the hypothesis of physical or structural damage at macroscopic scales is unlikely to play a role in this study.

Besides of fundamental interest, inverse dependence of skin permeability on contact area also has practical implications. Specifically, we predicted that an array of reservoirs should deliver more drug compared to that from a single reservoir. Although the contact area is reduced by using an array, skin permeability underneath each reservoir in the array is expected to be higher than that observed from a single large reservoir. If the fraction of the total skin area occupied by the reservoirs in the array is, α, then the effective permeability induced by the array, P_{array}, is given by the following equation.

$$P_{array} = \alpha P \quad [9]$$

where, P is permeability of skin underneath each reservoir of a given size. Depending on the values of α and P significant enhancements of skin permeability can be obtained.

To experimentally determine the enhancement obtained by reservoir arrays, we created patches holding reservoir arrays containing ^{3}H labeled mannitol as the model solute. These patches were created at varying reservoir sizes (16 mm, 9 mm, 5 mm, and 3 mm). In these patches, the reservoirs were arranged in a square pattern with the center-to-center distance between two adjacent reservoirs equal to twice the reservoir diameter. The patches were placed on skin pieces possessing an area of 10.25 cm^2 atop Franz Diffusion cells (receiver volume 12 ml, diameter 16 mm) keeping the area fraction the same for all the reservoir sizes (~20%). With this configuration, the numbers of reservoirs that could be fitted in an area of 10.25 cm^2 were 1, 4, 10, and 28 for reservoirs possessing diameters of 16mm, 9 mm, 5 mm, and 3 mm, respectively. The reservoir packing fraction used is not necessarily the maximum or optimum packing fraction, but is chosen simply to demonstrate the principles. Figure 7 shows the amount of mannitol delivered per unit macroscopic area (i.e. 10.25 cm^2) from arrays of various diameter reservoirs. A 3 mm reservoir array delivers about 11 times more mannitol than that from a 16 mm reservoir containing an identical formulation. Once again, the actual magnitude of the enhance-

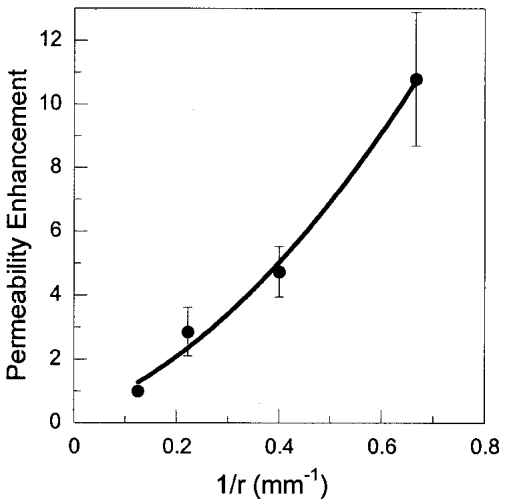

Fig. 7. Drug delivery enhancement obtained by using an array of reservoirs of different sizes. The amount of mannitol delivered into the skin increases with a decrease in the reservoir size. All enhancements are obtained by normalizing the amount delivered into the skin at any particular reservoir size to that delivered from a 16 mm reservoir. Error bars correspond to one standard deviation (n = 5).

ment depends on the size and geometry of the skin used in the experiments. However, the data shown in Fig. 7 confirm that an array of reservoirs enhances skin permeability compared to that obtained from a single large reservoir.

The data and analysis presented in this study show that a simple modification of the drug dispensing geometry can lead to quantitative enhancement of transdermal transport. In light of the constraints in delivering large quantities of drugs across the skin, these "array patches" should be investigated in future studies. Future studies should specifically focus on assessing whether the enhancement due to arrays is also observed *in vivo* and if the enhancement factors scale similarly.

ACKNOWLEDGMENTS

The authors thank Richard Keeler for technical assistance.

REFERENCES

1. A. Bouwstra. The skin, a well organized membrane. *Coll. Surf. A*. **123-124**:403–413 (1997).
2. S. Mitragotri. Synergistic effect of enhancers for transdermal drug delivery. *Pharm. Res.* **17**:1354–1359 (2000).
3. S. Mitragotri, D. Blankschtein, and R. Langer. Ultrasound-Mediated Transdermal Protein Delivery. *Science* **269**:850–853 (1995).
4. A. V. Badkar and A. K. Banga. Electrically enhanced transdermal delivery of a macromolecule. *J. Pharm. Pharmacol.* **54**:907–912 (2002).
5. C. B. Finnin and M. T. Morgan. Transdermal penetration enhancers: Applications, limitations and potential. *J. Pharm. Sci.* **88**:955–958 (1999).
6. Y. S. Papir, K. Hsu, and R. H. Wildnauer. The mechanical properties of stratum corneum. I. The effect of water and ambient temperature on the tensile properties of newborn rat stratum corneum. *Biochim. Biophys. Acta* **399**:170–180 (1975).
7. L. Norlen, A. Emilson, and B. Forslind. Stratum corneum swelling. Biophysical and computer assisted quantitative assessments. *Arch. Dermatol. Res.* **289**:506–513 (1997).
8. B. Van Duzee. The influence of water content, chemical treatment and ambient temperature on rheological properties of skin. *J. Invest. Dermatol.* **71**:140–144 (1978).
9. G. B. James, B. Jemec, B. I. Jemec, and J. Serup. The effect of superficial hydration on mechanical properties of skin in vivo: implications for plastic surgery. *Plast. Reconstr. Surg.* **85**:100–103 (1990).
10. A. Alonso, N. Meirelles, V. Yushmanov, and M. Tabak. Water increases the fluidity of intercellular membranes of stratum corneum: Correlation with water permeability, elastic and electrical resistance properties. *J. Invest. Dermatol.* **106**:1058–1063 (1996).
11. T. Yamamura and T. Tezuka. The water holding capacity of the stratum corneum measured by ^{1}H-NMR. *J. Invest. Dermatol.* **93**: 160–164 (1989).
12. L. Pedersen and G. Jemec. Plasticising effect of water and glycerin on human skin *in vivo*. *J. Dermatol. Sci.* **19**:48–52 (1999).
13. I. H. Blank. Further observations on factors which influence the water content of the stratum corneum. *J. Invest. Dermatol.* **21**: 259–271 (1953).
14. E. Sparr and H. Wennerstrom. Responding phospholipid membranes-interplay between hydration and permeability. *Biophys. J.* **81**:1014–1028 (2001).
15. D. A. Van Hal, E. Jeremiasse, H. E. Junginger, F. Spies, and A. Bouwstra. Structure of Fully Hydrated Human Stratum Corneum—a freeze fracture electron microscopy study. *J. Invest. Dermatol.* **106**:89–95 (1996).
16. M. Buchanan, J. Arrault, and M. Cates. Swelling and dissolution Lamellar phases: role of bilayer organization. *Langmuir* **14**:7371–7377 (1998).
17. S. Diridollou, F. Patat, F. Gens, L. Vaillant, D. Black, J. Lagarde, Y. Gall, and M. Berson. *In vivo* model of the mechanical properties of the human skin under suction. *Skin Res. Technol.* **6**:214–221 (2000).
18. M. Walser. Role of edge damage in sodium permeability of toad bladder and a means of avoiding it. *Am. J. Phys.* **219**:252–255 (1970).
19. S. Helman and D. A. Miller. Edge damage effect on electrical measurements of frog skin. *Am. J. Phys.* **225**:972–977 (1973).
20. S. Helman and D. A. Miller. Edge damage effect on measurement of urea and sodium flux in frog skin. *Am. J. Phys.* **226**:1198–1203 (1974).